



# Application Note

## Energy Harvesting for LTE-M Based Applications

### **Abstract:**

This document presents a feasibility study on using solar energy harvesting for Wireless Sensor Nodes based on LTE-M communication. The main objective is to use commercially available PV cells to make Wireless Sensor Node based applications energy autonomous. This document is based on Nowi's own Blue Coral Development Platform. More information on the platform and the reference design files can be found on the Nowi website.



## Table of Contents

<b>1. Introduction</b>	3
<b>2. Applications</b>	3
<b>3. System Architecture</b>	3
<b>4. Power Management</b>	4
4.1 Indoor Solar Harvesting	4
4.2 Outdoor Solar Harvesting	5
4.3 Overcharge Protection	5
<b>5. Energy Harvesting Measurements</b>	6
5.1 Indoor Battery Charging	6
5.2 Outdoor Battery Charging	7
<b>6. System Power Consumption</b>	8
6.1 Current Profile nRF9160	8
6.2 Average Power Consumption Table	9
6.3 System Energy Autonomy	9
<b>7. Conclusion</b>	9

## Application Note

# Energy Harvesting for LTE-M Based Applications

### 1. Introduction

There is photovoltaic energy present in indoor and outdoor environments. This photovoltaic energy can be harvested to power low-power IoT devices such as wireless sensor nodes.

We can summarize the main points of this application as follows: Both indoor and outdoor solar harvesting could be applied to power low-power cellular connected devices.

### 2. Applications

Connected smart sensors are becoming an increasingly popular topic within the internet of things applications. Virtually anything contains multiple sensors that send their data to the cloud using wireless communication. There are a variety of applications in the cellular IoT space where solar energy harvesting can be implemented to increase battery lifetime or to achieve energy autonomy. Typically these applications include one or more sensors and a cellular communication chipset that operates in PSM (Power Saving Mode). Examples of these applications are asset tracking, wireless sensor networks, and smart sensor systems.

### 3. System Architecture

This section presents the system architecture of a wireless sensor node based on cellular communication.

Figure 1 shows the system architecture of a wireless sensor node, this architecture is based on the design of the Nowi Blue Coral Development Board. Typically a wireless sensor network includes multiple of these wireless sensor nodes.

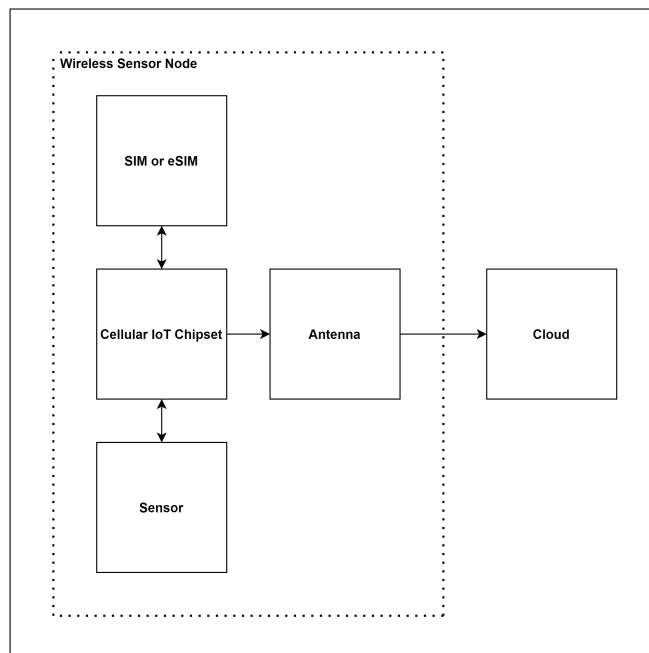


Figure 1: System Architecture LTE-M WSN

The system architecture is based on Nordic Semiconductors nRF9160 cellular IoT chipset. This chipset includes an ARM Cortex-M33 based CPU which is capable of sampling sensor data either from digital sensors through the SPI (Serial Peripheral Interface) or I2C (Inter-Integrated Circuit), or sampling sensor data from analog sensors using one of the analog capable GPIOs.

For the cellular communication either a regular SIM (Subscriber Identification Module) or eSIM (embedded Subscriber Identification module) can be used. eSIM allows the user to shrink down size by using MFF2 type SIM instead of 4FF type SIM. eSIM also allows the user to use multiple providers on a single SIM, where regular SIM limits to just one provider.

In order to establish a connection to the LTE-M network, a cellular IoT chip requires an antenna that supports the frequency bands specified by LTE-M. The cellular device typically operates in PSM (Power Saving Mode) to decrease power consumption, in this operating mode typically only uplink communication is possible. The sensor data is then sent to the cloud using this antenna, and in the cloud it is possible to perform post-processing or show data in a dashboard.

#### 4. Power Management

This section presents the power management in a solar powered LTE-M wireless sensor node based on Nowi's NH2D0245 energy harvesting PMIC.

Both in indoor and outdoor environments there is solar energy present. The amount of energy that can be harvested depends on the illuminance and the type of PV panel used. For the PMIC we are using NH2D0245, and we are charging a Lithium-Polymer based secondary battery. The NH2D0245 boost converter can boost 2 or 2.3 times which is selected by the MPPT algorithm.

##### 4.1. Indoor Solar Harvesting

Figure 2 shows a typical configuration with the NH2D0245 for indoor solar harvesting. As shown, the range bits in pins 9 to 11 and PWRS are all set to **GND**. By configuring the range bits and PWRS to **GND**, the PMIC is optimized more for lower power operation, which is typical for indoor solar harvesting.

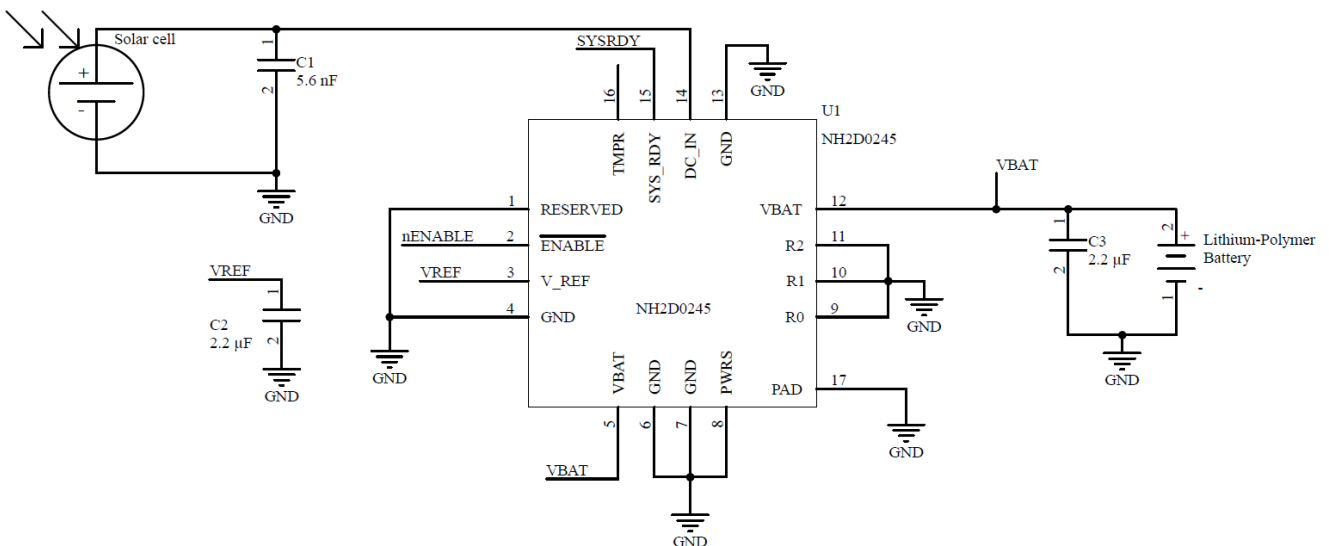


Figure 2: Indoor Solar Harvesting Configuration

For indoor solar harvesting the solar cell used is the AM-1454 amorphous silicon solar cell from manufacturer Panasonic. This solar cell is optimized for indoor environments. The battery used is a 800 mAh Lithium-Polymer chemistry battery from the manufacturer BAK.

### 4.2. Outdoor Solar Harvesting

Figure 3 shows a typical configuration with the NH2D0245 for outdoor solar harvesting. As shown, the range bits in pins 9 to 11 and PWRS are all set to **VBAT**. By configuring the range bits and PWRS to **VBAT**, the PMIC is optimized more for higher power operation, which is typical for outdoor solar harvesting.

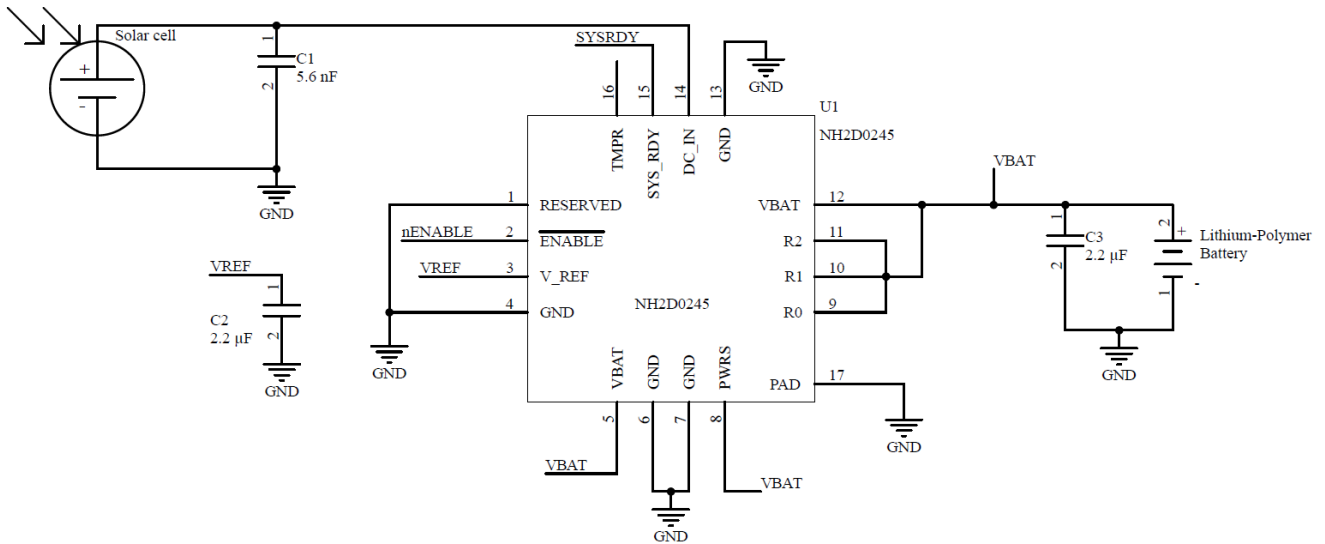


Figure 3: Outdoor Solar Harvesting Configuration

For outdoor solar harvesting the solar cell used is the AM-5308 amorphous silicon solar cell from manufacturer Panasonic. This solar cell is optimized for outdoor environments. The battery used is a 800 mAh Lithium-Polymer chemistry battery from the manufacturer BAK.

### 4.3. Overcharge Protection

The  $\overline{\text{ENABLE}}$  pin of the NH2D0245 can be used as a means of overcharge protection. By toggling this pin you can enable or disable conversion, which results in enabling or disabling the battery being charged. By disabling conversion when the battery voltage passes a threshold, the battery will stop charging, and effectively will be a form of overcharge protection.

## 5. Energy Harvesting Measurements

This section presents measurements of solar energy harvesting with the NH2D0245 in indoor and outdoor environment based on the configurations shown in figure 2 and 3. In both test setups the battery being charged is of Lithium Polymer chemistry.

### 5.1. Indoor Battery Charging

The light spectrum of indoor light used in the battery charging test is shown in Figure 4, the dominant source of light is of fluorescent type. The illuminance is equal to approximately 685 Lux.

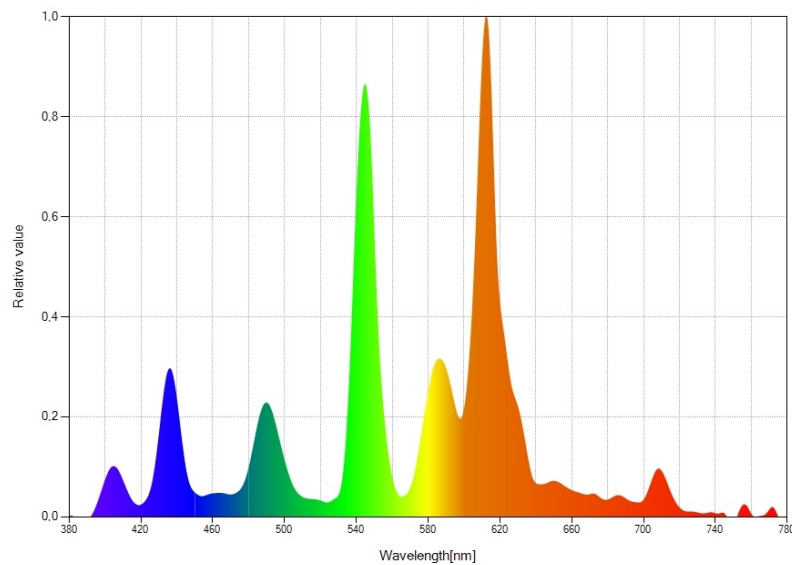


Figure 4: Spectrum Indoor Light

The battery charging current for three Panasonic AM1454 configured in parallel, under the light circumstances shown in figure 4 is shown in figure 5. The average battery charging current is equal to approximately 136  $\mu\text{A}$ , the battery voltage is equal to approximately 4 V. The peaks that go downwards in the current correspond to the maximum power point tracker interval of approximately one second.

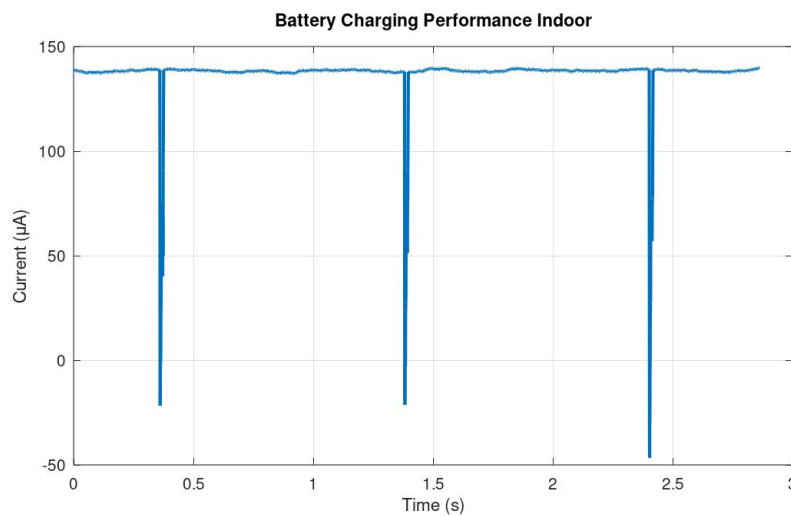


Figure 5: Indoor Battery Charging Current

## 5.2. Outdoor Battery Charging

The light spectrum of outdoor light used in the battery charging test is shown in Figure 6, the dominant source of light is of fluorescent type. The illuminance is equal to approximately 88600 Lux.

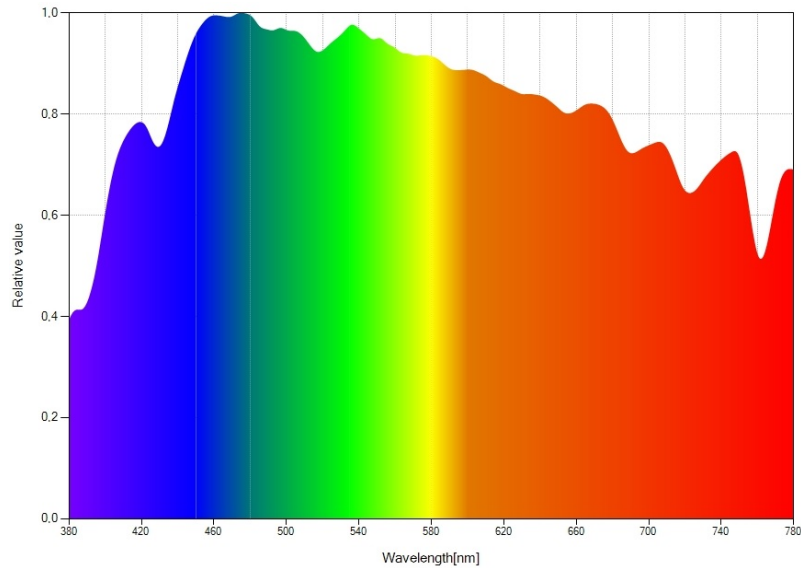


Figure 6: *Spectrum Outdoor Light*

The battery charging current for one Panasonic AM5308, under the light circumstances shown in figure 6 is shown in figure 7. The average battery charging current is equal to approximately 310  $\mu$ A, the battery voltage is equal to approximately 4 V. The peaks that go downwards in the current correspond to the maximum power tracker interval of approximately one second.

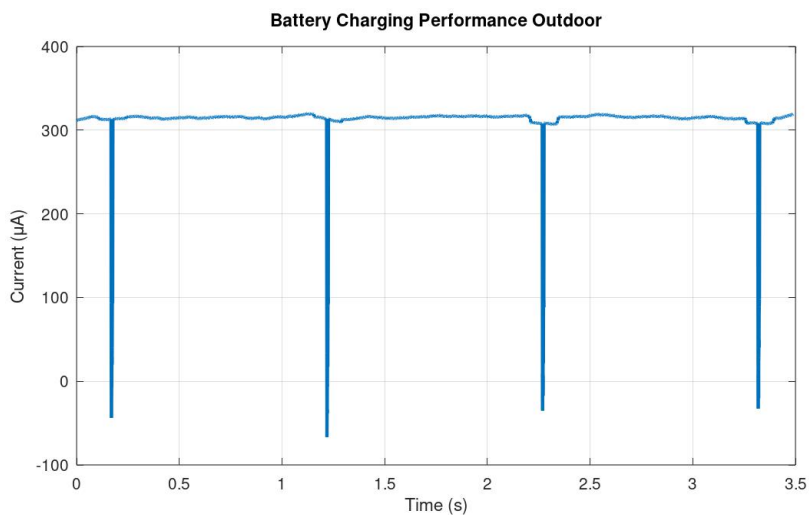


Figure 7: *Outdoor Battery Charging Current*

## 6. System Power Consumption

This section presents the current profile of a LTE-M message based on UDP of the nRF9160 SiP. This section also covers the average consumption based on different geographical locations.

### 6.1. Current Profile nRF9160

Figure 8 shows the current profile of the nRF9160 when sending a UDP message of approximately 1kB. This current profile is based on the Nordic Online Power Profiler tool. During this message event the total consumed energy is approximately 0.37 Joule.

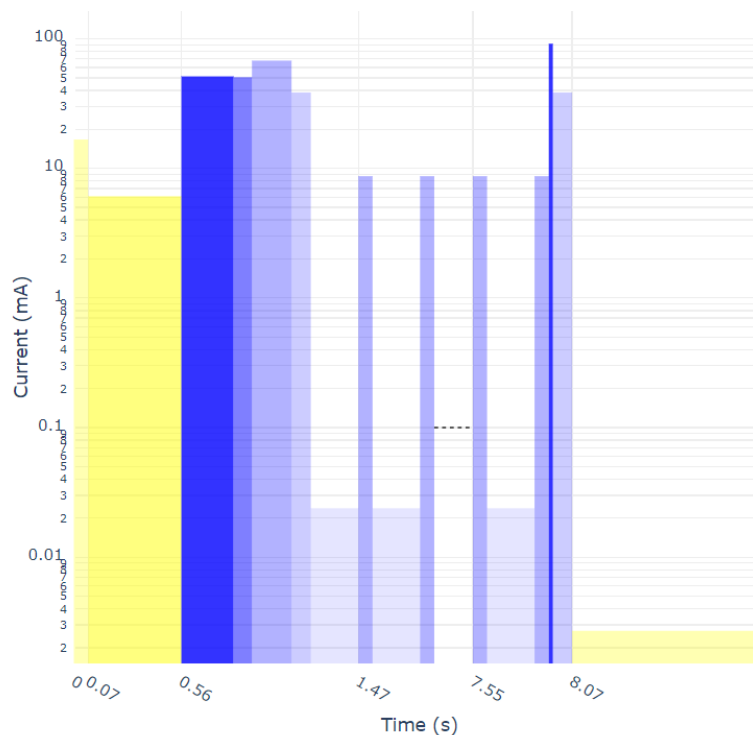


**Figure 8:** Current Profile LTE Event

The first two yellow peaks correspond to the device synchronizing with the network and the SIM.

The four dark blue and light blue peaks after this correspond to the device setting up the RRC protocol, performing a Tracking Area Update and sending data to the cloud.

The repetitive small and large peaks that come after this correspond to the cDRX idle and cDRX events.

The final light blue peak indicates the device executing the DRX inactivity timer, and the yellow current at the end of the current profile in figure 8 correspond to the device going into sleep or Power Saving Mode. The floor current here is equal to 2.7  $\mu$ A.



## 6.2. Average Power Consumption Table

Table 1 shows numbers of average power consumption of the nRF9160 SiP based on different geographical locations. These average consumption values are based on the simulation in the Nordic Online Power Profiler for LTE. In the Online Power Profiler tool, revision 2 of the nRF9160 is selected. In the Online Power Profiler tool, LTE-M is selected as the communication protocol and operating in PSM, Power Saving Mode, is enabled. The average consumption values are based on a message interval of one hour with a payload of 1 kB. The online Power Profiler Tool uses the UDP example code provided by Nordic Semiconductor.

**Table 1:** Average Power Consumption for Different Geographical Locations

Location	Network Operator	Average consumption* [ $\mu$ A] @3.7V
Finland	DNA	31
Japan	Docomo	31
Norway	Telenor	43
US	Verizon	24

\* Based on the Online Power Profiler tool.

## 6.3. System Energy Autonomy

As shown in table 1, the average power consumption at 3.7 V varies between 24  $\mu$ A and 43  $\mu$ A based on the geographical location of the wireless sensor node. Different geographical locations have different power consumption for the same message interval and message payload. This is because each network operator has its own network settings, which result in slightly different power consumption.

When comparing the average power consumption values in table 1 with the average battery charging current values of the measurements in figure 5 and figure 7, we see that the average charging current is larger than the average consumption. For the application in an indoor environment there is approximately a headroom of  $\pm 100 \mu$ A and for the application in an outdoor environment there is approximately a headroom of  $\pm 270 \mu$ A.

## 7. Conclusion

As shown in the measurements in this document, for indoor solar harvesting, the average battery charging current is equal to 136  $\mu$ A. For outdoor solar harvesting, the average battery charging current is equal to 310  $\mu$ A. These battery charging currents allow for a headroom of respectively  $\pm 100 \mu$ A and  $\pm 270 \mu$ A when compensating for the consumption of transmitting data with the nRF9160 cellular IoT SiP.

This headroom allows to either increase the consumption of the system or to decrease the size of the PV harvester, while still maintaining energy autonomy. The consumption of the system can be increased by powering additional sensors like environmental sensors, or to decrease the message interval and increase the message payload by sending more data. One alternative approach can be to decrease the size of the PV harvester, while still maintaining plug and forget for the cellular IoT solution.